A Nonlinear Elimination Preconditioned Newton Method with Applications in Arterial Wall Simulation*

Shihua Gong and Xiao-Chuan Cai

Abstract Arterial wall can be modeled by a quasi-incompressible, anisotropic and hyperelastic equation that allows large deformation. Most existing nonlinear solvers for the steady hyperelastic problem are based on pseudo time stepping, which often requires a large number of time steps especially for the case of large deformation. It is also reported that the quasi-incompressibility and high anisotropy have negative effects on the convergence of both Newton's iteration and the linear Jacobian solver. In this paper, we propose and study a nonlinearly preconditioned Newton method based on nonlinear elimination to calculate the steady solution directly without pseudo time integration. We show numerically that the nonlinear elimination preconditioner accelerates Newton's convergence in cases with large deformation, quasi-incompressibility and high anisotropy.

1 Introduction

Some biological soft tissues, such as the arterial wall, are quasi-incompressible and are reinforced by collagen fibers, which induce the anisotropy in the mechanical response. Polyconvex hyperelastic models [2, 4], which are based on polyconvex energy-stored functions, provide a unified framework to describe the quasi-incompressibility, the anisotropy and the nonlinearly elastic behavior of arterial walls in the regime allowing large deformations. By using finite element discretiza-

S. Gong
Beijing International Center for Mathematical Research, Peking University, Beijing 100871, P. R. China, e-mail: gongshihua@pku.edu.cn

X.-C. Cai
Department of Computer Science, University of Colorado Boulder, Boulder, CO 80309, USA, e-mail: cai@cs.colorado.edu

* The work of the first author was supported by National Natural Science Foundation of China (NSFC) (Grant No.91430215).

tions [3] for these models and Newton-type nonlinear solvers, numerical simulation of arterial walls becomes a promising approach in clinical diagnosis and treatment assistance. However, the design of robust nonlinear and linear solvers is a challenging problem due to the sophisticated mechanical properties of arterial walls.

In [5], the authors consider several material models for arterial walls in order to study the mechanical response and the influence on the nonlinear iteration as well as on the finite element tearing and interconnecting-dual primal (FETI-DP) iterative linear solver. The stagnation of Newton's method is observed for some parameter sets. In order to cope with the quasi-incompressible condition, an augmented Lagrange approach is proposed in [6]. The penalty parameter for the incompressibility can be chosen much smaller and therefore the resulting linear systems have better properties. Both nonlinear solvers mentioned above are based on pseudo time stepping, which often requires a large number of global nonlinear iterations especially for the case of large deformation.

To accelerate the convergence of the nonlinear iteration, we consider a nonlinearly preconditioned Newton method based on nonlinear elimination to calculate the solution directly without pseudo time integration. The nonlinear elimination method is first proposed and analyzed in [12] and then developed in [7, 11] for the problems with high local nonlinearity. For our cases of hyperelasticity, we numerically observe that the variables with stronger nonlinearity are not fixed, but change as the propagation of the elastic wave. Thus, we adaptively detect the variables and equations with stronger nonlinearity by the residuals. After eliminating these equations, the approximate solution is more accurate in some key locations of the elastic wave and therefore the global Newton's method converges better.

2 Modeling and Discretization

In this section, we discuss a hyperelastic model for arterial walls and its finite element discretization. First, we introduce some basic notations in continuum mechanics. The body of interest in the reference configuration is denoted by $\hat{\Omega} \in \mathbb{R}^3$, parameterized in $\hat{x}$, and the current configuration by $\Omega \in \mathbb{R}^3$, parametrized by x. The deformation map $\phi : \hat{\Omega} \mapsto \Omega$ is a differential isomorphism between the reference and current configuration. The deformation gradient F is defined by $F(\hat{x}) = \nabla\phi(\hat{x})$ with the Jacobian $J(\hat{x}) = \det F(\hat{x}) > 0$. The right Cauchy-Green tensor is defined as $C = F^T F$.

The hyperelastic materials postulate the existence of a so-called store-energy function ψ, defined per unit reference volume. According to the axiom of material frame-indifference [8], the energy functional depends on the Cauchy-Green tensor, i.e., $\psi = \psi(C)$. The first and second Piola-Kirchhoff stress tensor can be derived as $P = FS, \quad S = 2\partial_C \psi(C)$. And then the Cauchy stress is given by $\sigma = J^{-1} FSF^T$. The balance of the momentum is governed by the following partial differential equation

$$\mathrm{div} P = -f,$$

plus appropriate boundary condition. Here f is the body force vector.

We focus on the polyconvex energy functional proposed in [4],

$$\begin{aligned}\psi_A &= \psi^{isochoric} + \psi^{volumetric} + \psi^{ti} \\ &:= c_1\left(\frac{I_1}{I_3^{1/3}} - 3\right) + \varepsilon_1\left(I_3^{\varepsilon_2} + \frac{1}{I_3^{\varepsilon_2}} - 2\right) + \sum_{i=1}^{2}\alpha_1\left\langle I_1 J_4^{(i)} - J_5^{(i)} - 2\right\rangle^{\alpha_2},\end{aligned} \tag{1}$$

which models the quasi-incompressible and fibre-enforcing arterial wall. Here, $\langle b\rangle$ denotes the Macaulay brackets defined by $\langle b\rangle = (|b|+b)/2$, with $b \in R$. And I_1, I_2, I_3 are the principal invariants of C; i.e. $I_1 := \mathrm{tr}C, I_2 := \mathrm{tr}[\mathrm{cof}\ C], I_3 := \det C$, where $\mathrm{cof}\, C = (\det C)C^{-T}$. The additional mixed invariants $J_4^{(i)}, J_5^{(i)}$ characterize the anisotropic behavior of arterial wall and are defined as $J_4^{(i)} := \mathrm{tr}[CM^{(i)}], \quad J_5^{(i)} := \mathrm{tr}[C^2M^{(i)}], \quad$ for $i = 1:2$, where $M^{(i)} := a^{(i)} \otimes a^{(i)}, i = 1,2$ are the structural tensors with $a^{(i)}, i = 1,2$ denoting the direction fields of the embedded collagen fibers.

The polyconvexity condition in the sense of [2] is the essential condition to ensure the existence of energy minimizers. There are three parts in ψ_A:

- $\psi^{isochoric}$ is the isochoric part of the isotropic energy. Similar to the Neo-Hookean material, c_1 is stress-type coefficient with upper and lower bounds.
- $\psi^{volumetric}$ is the penalty function to account for the quasi-incompressibility. The coefficients $\varepsilon_1, \varepsilon_2$ would be very large for the incompressible material.
- ψ^{ti} is the transversely isotropic part. The anisotropy comes from the exponential stiffening of the fibers when increasing loads are applied. Relative large coefficients α_1, α_2 indicate large anisotropy.

According to [3], the lowest-order Lagrange finite element with linear shape functions is not sufficient to provide a good approximation for the arterial wall stresses, whereas for the Lagrange finite elements or F-bar formulations with quadratic shape functions, suitable results are obtained. Instead of concerning about the stress, we focus on the nonlinear solvers for the resulting system. Thus, for simplicity, we use the $\mathscr{P}_1$ Lagrange finite element to approximate the displacement.

3 Inexact Newton Method with Nonlinear Preconditioning

With a slight abuse of notation, we denote the nonlinear system after the discretization as described above

$$F(u^*) = 0$$

where $F : \mathrm{R}^n \mapsto \mathrm{R}^n$. Inexact Newton (IN) algorithms [9, 10] are commonly used for solving such system and can briefly be described here. Suppose $u^{(k)}$ is the current approximate solution, a new approximate solution $u^{(k+1)}$ can be computed through

$$u^{(k+1)} = u^{(k)} + \lambda^{(k)} p^{(k)},$$

where the inexact Newton direction $p^{(k)}$ satisfies

$$\|F(u^{(k)}) + F'(u^{(k)})p^{(k)}\| \leq \eta_k \|F(u^{(k)})\|.$$

Here $\eta_k \in [0,1)$ is a scalar that determines how accurately the Jacobian system needs to be solved, and $\lambda^{(k)}$ is another scalar that determines how far one should go in the selected direction.

3.1 Nonlinear Elimination

It is reported in [5, 6], the incompressibility and large anisotropy have a negative effect on the convergence of both Newton's iteration and the Jacobian solver. To accelerate Newton's convergence, we introduce a nonlinear elimination preconditioner [7, 11, 12], which balances the nonlinearity of the global problem by solving the subproblems defined in the subdomains or subspaces. Let $S = \{1, \cdots, n\}$ be an index set; i.e., one integer for each unknown u_i and residual F_i. We choose a subset $S_b \subset S$ of the indices corresponding to the "bad" degrees of freedom (d.o.f.), of which the nonlinearity is dominant. The corresponding subspace is denoted by

$$V_b = \{v \mid v = (v_1, \cdots, v_n)^T \in \mathrm{R}^n, v_k = 0, \text{ if } k \notin S_b\}.$$

The corresponding restriction operator is denoted by $R_b \in \mathrm{R}^{n \times n}$, whose kth column is either zero if $k \notin S_b$ or the kth column of the indentity matrix $I_{n\times n}$. Thus the subspace and the corresponding restriction for the "good" d.o.f. are denoted by V_g and $R_g = I_{n\times n} - R_b$.

Given an approximate solution u and a sub index set S_b, the nonlinear elimination algorithm finds the correction by approximately solving $u_b \in V_b$,

$$F_b(u_b) := R_b F(u_b + u) = 0. \tag{2}$$

The new approximate solution is then updated as $w = u_b + u$. It is easy to see that the Jacobian of the sub nonlinear problem (2) is $J_b(u_b) = R_b J(u_b + u) R_b^T$. Here $J = F' = \left(\frac{\partial F_i}{\partial u_j}\right)_{n\times n}$ is the Jacobian of F.

Suppose we are at the iteration k and $u^{(k)}$ is the current approximation, the inexact Newton algorithm with nonlinear elimination is described as below

---

Algorithm 1. (IN-NE)

Step 1. Compute the next approximate solution $u^{(k+1)}$ by solving the following nonlinear system

$$F(u) = 0$$

with one step of IN iteration using $u^{(k)}$ as the initial guess. If the global convergent condition is satisfied, stop. Otherwise, go to Step 2.

Step 2. (Nonlinearity checking)

2.1 If $\|F(u^{(k+1)})\| < \rho_1\|F(u^{(k)})\|$, go to Step 1.

2.2 Finding "bad" d.o.f. by

$$S_b := \{j \in S \mid |F_j(u^{(k+1)})| > \rho_2\|F(u^{(k+1)})\|_\infty\}.$$

And extend S_b to S_b^δ by adding the neighbor d.o.f..

2.3 If $\#(S_b^\delta) < \rho_3 n$, go to Step 3. Otherwise, go to Step 1.

Here $\rho_1, \rho_2, \rho_3 \in (0,1)$ and $\delta \in Z_+$ are pre-chosen constants.

Step 3. Compute the correction $u_b^\delta \in V_b$ by solving the sub nonlinear system approximately

$$F_b^\delta(u_b^\delta) := R_b^\delta F(u_b^\delta + u^{(k+1)}) = 0,$$

with an initial guess $u_b^\delta = 0$ and a relative tolerance $\text{tol} = \max(\gamma_a, \gamma_r\|R_b^\delta F(u^{(k+1)})\|)$. If $\|F(u_b^\delta + u^{(k+1)})\| < \|F(u^{(k+1)})\|$, accept the correction and update $u^{(k+1)} \leftarrow u_b^\delta + u^{(k+1)}$. Go to Step 1.

There are three tolerance parameters in the nonlinear checking step: ρ_1 is the tolerance for the reduction of the residual norm, ρ_2 is the tolerance to pick up the bad d.o.f. and ρ_3 is the tolerance to limit the size of the subproblem. In Step 3, we only accept the correction by nonlinear elimination if the residual norm decreases. But in practice, if the norm of the corrected residual does not decrease for 3 successive steps, we choose to accept the correction without checking the residual.

Different to the nonlinear elimination method proposed in [12], where the authors fix for all steps the set of equations to eliminate, we construct adaptively the index set S_b by the residual $F(u^{(k+1)})$. Actually, the residual can be viewed as a measurement of the Hessian of F by the Taylor expansion,

$$\begin{aligned} F(u^{(k+1)}) &= F(u^{(k)}) + F'(u^{(k)})p^{(k)} + \langle F''(u^{(k)} + \theta p^{(k)})p^{(k)}, p^{(k)}\rangle \\ &\approx \langle F''(u^{(k)} + \theta p^{(k)})p^{(k)}, p^{(k)}\rangle, \end{aligned}$$

since the Jacobian system is solved approximately. From this perspective, eliminating the equations with large residual is a way to control the higher order terms of F such that it can be linearly approximated much better during the global Newton iteration. However, the nonlinear elimination just on the equations with indices in S_b could lead to thrashing (i.e., the norm of the residual $\|F\|$ could become larger due to the boundary effect). To ease this phenomenon, we extend the index set S_b to S_b^δ by adding the neighbor d.o.f, of which the distances to S_b are smaller than δ.

4 Numerical Results

We implement the discretization for hyperelasticity and the nonlinear solvers described in the previous sections by using FEniCS [13] and PETSc [1], respectively. Based on the parameter sets of the model ψ_A in Table. 1, we propose three test examples to investigate the performance of nonlinear elimination for the materials with large deformation, quasi-incompressibility and high anisotropy. In all of the tests, the backtracking line search strategy is used to determine the maximum amount to move along the search direction computed by a direct solver.

Set	Layer	c_1	ε_1	ε_2(-)	α_1	α_2	Purpose
L	–	1.e3	1.e3	1.0	0.0	0.0	Deformations by different pulls
C1	–	1.e3	1.e3	1.0	0.0	0.0	Different penalties for compressiblity
C2	–	1.e3	1.e4	1.0	0.0	0.0	
C3	–	1.e3	1.e5	1.0	0.0	0.0	
A1	Adv.	7.5	100.0	20.0	1.5e10	20.0	Anisotropic arterial walls
	Med.	17.5	100.0	50.0	5.0e5	7.0	
A2	Adv.	6.6	23.9	10	1503.0	6.3	
	Med.	17.5	499.8	2.4	30001.9	5.1	
A3	Adv.	7.8	70.0	8.5	1503.0	6.3	
	Med.	9.2	360.0	9.0	30001.9	5.1	

Table 1: Model parameter sets [5, 6] of ψ_A

Example 1. This example simulates the deformations of a cylindrical rod by different pulls. We fix one end of the rod and then pull it down from the other end. The material parameters are given in Set L of Table 1. It is an isotropic model since $\alpha_1 = 0.0$. The deformations by three different pulls $L_1 = 1.e1$ Pa, $L_2 = 1.e2$ Pa and $L_3 = 1.e3$ Pa are plotted in Fig. 1b. The convergence history of the Newton iteration with nonlinear elimination (IN-NE) is shown in Fig. 1a. We compare the results with those obtained by using a standard inexact Newton (IN) method. The blue lines are for the IN-NE algorithm while the red lines for the IN method. As indicated by Fig. 1a, the nonlinear elimination method accelerates the convergence of the Newton iteration even for the case of large deformation.

Example 2. This example studies the performance of nonlinear elimination for the cases of different compressibility. The parameters are given in the sets C1,C2 and C3 of Table 1. For consistency with linear elasticity, $C_1 = \frac{\mu}{2}, \varepsilon_1 = \frac{\kappa}{2}$, where μ, κ are the shear and bulk modulus. The Poisson ratio can be computed by $\nu = \frac{3\kappa - 2\mu}{2(3\kappa+\mu)}$; see Table 2. We use the same setting of the geometry and the boundary conditions with that of the previous example. Fig. 2 shows the superiority of the nonlinear elimination in the quasi-incompressible case.

Example 3. We consider an artificial arterial segment with a plaque and fibre-enforcing layers. The problem setting, including the geometry and boundary conditions, originates from [5]. More precisely, a pressure of up to 24 kPa (< 180 mmHg)

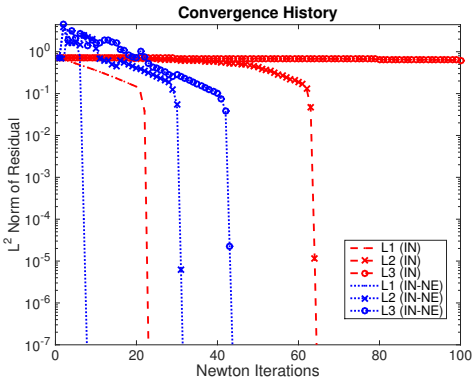

(a) Convergence history of IN and IN-NE

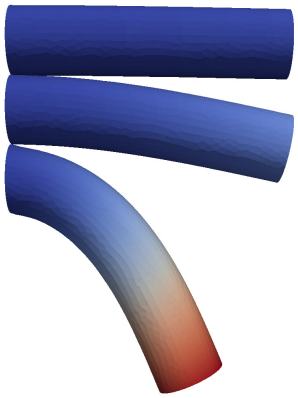

(b) Deformations by different pulls

Fig. 1: Numerical results of Example 1.

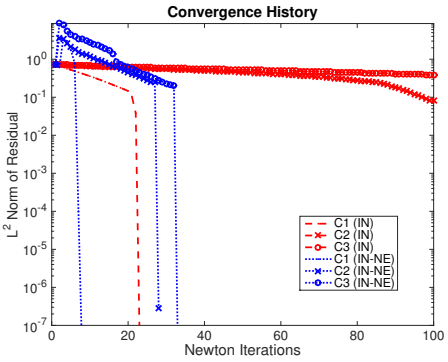

Fig. 2: Convergence histories for Example 2.

Set	Poisson's Ratio
C1	0.125
C2	0.452
C3	0.495

Table 2: Poisson's ratio of materials C1, C2 and C3.

is applied to the interior of the arterial segment, of which the von Mises stress is shown in Fig. 3b. The parameter sets A1 and A2 of Table 1 are adjusted in [5] to fit the experiment data, and A3 in [6] with slight modification. The convergence histories of IN and IN-NE are shown in Fig. 3b. Similar to the previous examples, the nonlinear elimination increases the residual at the first few steps of Newton's iteration, but then the iteration converges faster.

5 Conclusions

The main contribution of this paper was to investigate the performance of a nonlinear elimination preconditioner with applications in computational hyperelasticity.

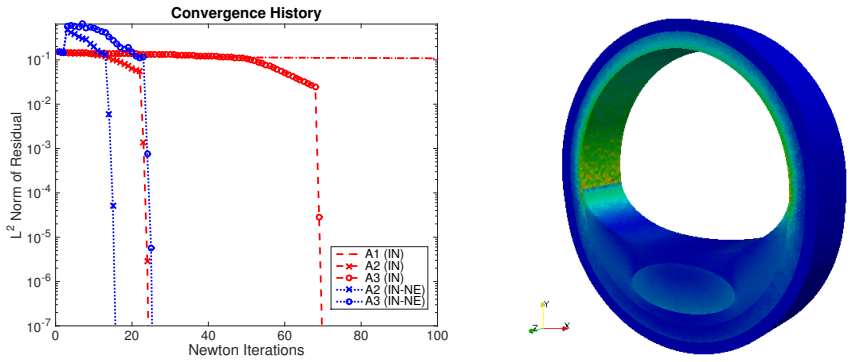

(a) Convergence histories of IN and IN-NE (b) von Mises stress

Fig. 3: Numerical result of Example 3.

A robust strategy of nonlinearity checking was adapted to capture the subregions with stronger nonlinearity, which coincide with the propagation of the elastic wave. Moreover, we found that the extension for the eliminating index set by adding the neighbor d.o.f. is an effective trick to ease the thrashing phenomenon of nonlinear elimination. As future work, we will use more feasible linear solvers for the Jacobian system and consider other arterial wall problems with patient-specific geometry.

References

1. S. Balay, S. Abhyankar, M. F. Adams, J. Brown, P. Brune, K. Buschelman, L. Dalcin, V. Eijkhout, W. D. Gropp, D. Kaushik, M. G. Knepley, L. C. McInnes, K. Rupp, B. F. Smith, S. Zampini, H. Zhang, and H. Zhang. PETSc users manual. Technical Report ANL-95/11 - Revision 3.7, Argonne National Laboratory, 2016.
2. J. M. Ball. Convexity conditions and existence theorems in nonlinear elasticity. *Arch. for Ration. Mech. Analysis*, 63:337–403, 1976.
3. D. Balzani, S. Deparis, S. Fausten, D. Forti, A. Heinlein, A. Klawonn, A. Quarteroni, O. Rheinbach, and J. Schröder. Numerical modeling of fluid–structure interaction in arteries with anisotropic polyconvex hyperelastic and anisotropic viscoelastic material models at finite strains. *Int. J. Numer. methods Biomed. Eng.*, 2015.
4. D. Balzani, P. Neff, J. Schröder, and G. A. Holzapfel. A polyconvex framework for soft biological tissues. Adjustment to experimental data. *Int. J. Solids Struct.*, 43:6052–6070, 2006.
5. D. Brands, A. Klawonn, O. Rheinbach, and J. Schröder. Modelling and convergence in arterial wall simulations using a parallel FETI solution strategy. *Comput. Methods Biomech. Biomed. Eng.*, 11:569–583, 2008.
6. S. Brinkhues, A. Klawonn, O. Rheinbach, and J. Schröder. Augmented Lagrange methods for quasi-incompressible materials–Applications to soft biological tissue. *Int. J. Numer. methods Biomed. Eng.*, 29:332–350, 2013.
7. X.-C. Cai and X. Li. Inexact Newton methods with restricted additive Schwarz based nonlinear elimination for problems with high local nonlinearity. *SIAM J. Sci. Comput.*, 33:746–762, 2011.

8. P. G. Ciarlet. *Mathematical Elasticity, Vol. I : Three-Dimensional Elasticity.* Series "Studies in Mathematics and its Applications". North-Holland, Amsterdam, 1988.
9. R. S. Dembo, S. C. Eisenstat, and T. Steihaug. Inexact Newton methods. *SIAM J. Numer. Analysis*, 19:400–408, 1982.
10. S. C. Eisenstat and H. F. Walker. Globally convergent inexact Newton methods. *SIAM J. Optim.*, 4:393–422, 1994.
11. J. Huang, C. Yang, and X.-C. Cai. A nonlinearly preconditioned inexact Newton algorithm for steady state lattice Boltzmann equations. *SIAM J. Sci. Comput.*, 38:A1701–A1724, 2016.
12. P. J. Lanzkron, D. J. Rose, and J. T. Wilkes. An analysis of approximate nonlinear elimination. *SIAM J. Sci. Comput.*, 17:538–559, 1996.
13. A. Logg, K.-A. Mardal, and G. Wells. *Automated solution of differential equations by the finite element method: The FEniCS book*, Volume 84. Springer Science & Business Media, 2012.